

Simulation Of Diffusion-Limited Aggregation Of Pectin

Abstract: *End-to-end diffusion-limited aggregation of an ideal, monodisperse pectin species with variable probability of intermolecular crosslinking has been simulated on a lattice. The aggregate was fixed on the lattice as a structure of segmented rods. The growth of averages of size, length, width, and radius of gyration followed a power law dependence on time as measured by number of random lattice movements of diffusing monomer. The structures exhibited multifractal properties that arise from both the diffusion process and the random generation of crosslinking sites. The growth of the average length of the structures was independent of probability of crosslinking under the condition of constant presence of diffusing monomer. The growth of the average size of the structures was directly related to the growth of the average number of crosslinks. Average length, width, and radius of gyration were related to growth of average size by power laws. Macintosh and IBM PC source code and executables are included on disk in this issue.*

INTRODUCTION

Mandelbrot has pioneered the application of fractal geometry to the description of many properties of natural systems.¹ A growing number of reports in the literature have described fractal properties of assemblies of macromolecules whose formation is influenced by a random process such as diffusion by Brownian motion.²⁻¹⁰ In general, fractal geometrical structures of such macroassemblies have properties that relate to each other by power laws. Computer simulations of diffusion-limited processes can generate large numbers of such structures so that statistical properties can be determined and compared to properties of assemblies of macromolecules that have been experimentally measured. Fractal geometry offers an opportunity to expand our fundamental concepts of the forms that macromolecular assemblies can assume.

Diffusion-Limited Aggregation

Fractal properties of simulated diffusion-limited aggregates were first reported by Witten and Sander.⁷ Their approach was to place in the middle of a lattice a seed particle. Next a new particle was introduced onto the lattice and was allowed to randomly walk from lattice point to lattice point until it reached a site that neighbored the seed particle. The new particle was then immobilized to become part of the aggregate. New particles were

introduced in like manner and the aggregate was allowed to grow. This simulation has provided new information on complex systems that have in the past resisted exact mathematical analysis. The structures generated had forms similar to those observed for gold aggregates^{8,9} and for diffusion-limited electrodeposits of zinc.¹⁰

Pectin

Pectin is a complex polysaccharide that consists of poly- α -(1 \rightarrow 4)-galacturonopyranosyl chains linked by at least one α -(1 \rightarrow 2)-rhamnopyranosyl group, to which pendant short chains of neutral sugars such as galactose and arabinose may be attached.¹¹ Pectin exhibits a variable content of neighboring methylated carboxyl groups.¹² Pectins aggregate and can produce two types of gels. At low pH high methoxy pectins form strongly hydrogen-bonded gels.¹³ At neutral pH, pectins that are more than 40% de-esterified form gels in the presence of divalent cations such as calcium.⁴⁻¹⁵ One of the roles of pectin in some plants is to provide flexible, hydrated structure to the middle lamella of the plant cell wall as a calcium pectate gel.¹⁶ Calcium pectate gels are believed to form by consecutive and cooperative intermolecular calcium salt bridges between carboxylate groups within polygalacturonyl blocks that have been described as junction zones.¹⁷ Motion about the α -(1 \rightarrow 4)-galacturonopyranosyl-glycosidic bond is restricted; this imposes a rigid rod-like conformation on pectin.^{11,18} The α -(1 \rightarrow 2)-glycosidic bond of interspersed rhamnopyranosyl groups abruptly redirects the polymer backbone, so that pectin currently can be viewed as a rod segmented by "kinks".¹⁹ Recent reports have suggested that pectin can form bundles of end-to-end aggregated chains.^{20,21}

For initial investigations, a simulation of pectin aggregation was designed in which both chain elongation and chain crosslinking were allowed. A diffusing "random walker" was chosen to represent an idealized pectin monomer that has three areas along the chain for interactions. These areas are analogous to the junction zones described by Rees.¹¹ The simulated aggregate can be viewed as a collection of oligomers joined together by crosslinks.

IMPLEMENTATION

General Approach

A seed monomer was fixed in the middle of a large square lattice mapped to a two dimensional array to begin the simulated aggregate. Each of three interaction sites (junction zones) was represented by a number in the array that corresponded to either a terminal (east and west) sites or an interior (north or south) crosslinking site (Fig. 1). A new pectin monomer was randomly placed on the lattice and was allowed to move to any of four neighboring points. To maintain consistency with earlier descriptions of diffusion-limited aggregation, this new monomer is called a "random walker". After each move the content of each new neighboring lattice point was examined for the presence of aggregate. If a terminal site was encountered, a terminal interaction was allowed; if a crosslinking site was encountered a crosslinking interaction was allowed. The new monomer was then fixed to the aggregate by the appropriate interaction. In the case of a terminal link, the orientation of the added monomer was allowed to vary so that a new crosslinking site had a set probability of forming (Fig. 1). This allowed the probability of crosslinking to be controlled. Adjoining junction sites of the added monomer were allowed to vary one unit in the north-south direction to represent a rod segmented by "kinks" (Fig. 1). Additional monomers were added one at a time. A few rules were prescribed to allow internal loops within the aggregate and to reject attachment at "sterically hindered" sites. These rules were similar in approach to those employed in cellular automata. These simulations also provided for termination of chain growth whenever an end of an attached monomer approached an existing chain by one lattice point. Attaching monomers were also allowed to bridge existing chains whose nearest ends were separated horizontally by one monomer length and vertically by no more than one lattice point.

Diffusion-limited aggregation of pectin

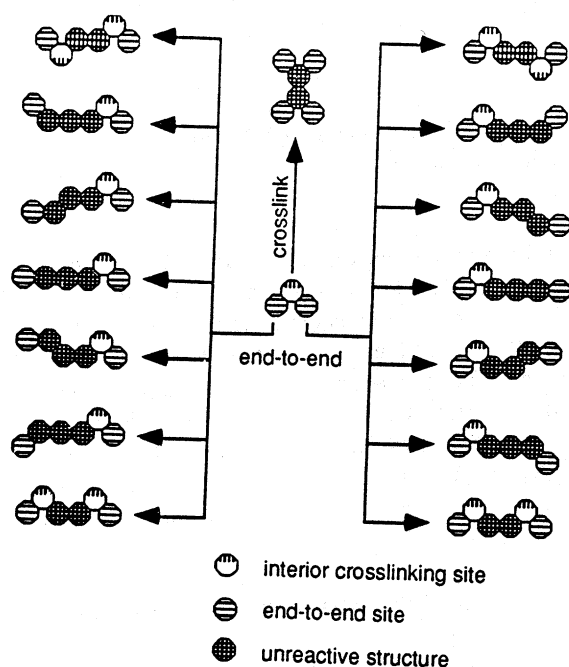


Fig. 1. Allowed orientations for monomer that attaches end-to-end. Crosslinking p corresponds to ratio of program selections of 4 end-to-end orientations that generate new potential crosslinking sites to selections of 10 end-to-end orientations that do not permit crosslinking.

To reduce the real computer time required for this simulation, the area of the random walker and the aggregate was restricted to within a bounding circle. A random walker, destined to attach itself to the aggregate, would, in its random walk from afar, have to pass through some random point on any circle drawn around the aggregate. The aggregate was grown in the center of a lattice that was mapped to an array of variables of the byte type. In the case of the 68881 coprocessor version, the aggregate was recentered in the array whenever growth of the structure extended beyond either the current east-west or north-south limits. The radius of the bounding circle was 12 points longer than the maximum distance of growth from the center towards the east. The random walker was launched at a random point along a concentric circle whose radius was 3 lattice units less than that of the bounding circle.²² A random radian angle, A , was generated within the range of 0 to 2π , and the lattice point for the launch point of the random walker was then calculated with the following equations :

$$\begin{aligned}
 r &= \text{radius of bounding circle} - 3 \\
 x &= \text{round}(r \cos(A)) \\
 y &= \text{round}(r \sin(A))
 \end{aligned}
 \quad \{A \text{ in } 0..2\pi\}$$

By having one new monomer always moving within this circle, a kind of constant chemical potential was maintained. Whenever the random walker encountered the bounding circle, it was instructed to bounce back, since this maintained randomness and required less computer time than allowing it to die and then be regenerated at a new launch site.

The unit of time is defined as the movement of the random walker from one lattice point to another. This time unit can be related to real time by the physical dimensions of the pectin monomer and its diffusion coefficient. Since Brownian motion has a dimension of two in a plane, the unit of time within a bounding circle of radius r was related to time within the largest circle (radius R) allowed by the array:

$$t = R * R / r * r$$

In this report time is measured in terms of "megevents", which is a unit assigned the value of a million random walker-movements on the lattice within the bounding circle.

Programming

Turbo Pascal was used for the IBM compatible PC version and Lightspeed Pascal was used for the Macintosh version. A 230 x 230 array (52,900 bytes) was first used to keep within the 64K limits for early versions of Turbo Pascal. The method of Porter²³ for allocating dynamic memory for a 720 x 720 array using pointer variables was adopted for a 2 megabyte Macintosh II. The random number generator was reseeded at the beginning of each random walk to avoid periodicity of paths. The orientation of a monomer attached end-to-end to the aggregate was selected by a random number tied to a case statement that allowed 7 states (Fig. 1).

The range of this random number mapped the set of numbers associated with a Pascal case statement and was used to control the probability of crosslinking (Table 1). The user is prompted for the number of simulations and for the duration, in terms of megevents, for each simulation. The following properties were averaged:

Size. The total number of monomers in the structure.

Length. The number of monomer lengths between the horizontal (east-west) extremities of the structure.

Width. The number of array elements between the vertical (north-south) extremities (maximum row element - minimum row element + 1) of the structure.

Crosslinks. The number of paired column elements that link chains within the structure.

R_g. The radius of gyration calculated from the root mean square distance of each structure-element from the center of gravity (Flory²⁴).

Chain. A continuous string of monomers joined end-to-end.

Time. Measured in megevents. One megevents = one million random movements within bounding circle and adjusted to size of bounding circle by equation 1.

Files

The properties of each simulated structure were stored in tab separated fields in one line appended to a text file so that the data could be imported into spreadsheet programs or examined directly by a text file editor. Both IBM and Macintosh versions of the program prompt the user for filenames. The Macintosh version also collects chain length frequency, distributions of length, crosslinks, and R_g, and real simulation time in a separate text file. A text file, 'AREAS.TXT' (IBM), or 'Array.Areas' (MAC), that contains the number of array elements within each bounding circle must be in the same directory or folder as the program file. The MAC program creates a log file to track the parameters and files generated by the program. Currently, the MAC program runs only under the Finder. Both executable files and Pascal source code files are included on disk. Updates are available from the author.

Hardware

Personal computers: Leading Edge Model D, AT&T PC 4300, Texas Instrument Professional, Telex 1280 AT, Macintosh SE, and Macintosh II.

A Daynafile 5.25", 360K, 3.5", 720K external dual drive was used to exchange data on Macintosh or IBM formatted diskettes.

Table 1. Orientation selection. The orientation for the monomer attached end-to-end was selected by a random number within the indicated range of numbers assigned to a Pascal case statement.

Orientation	Crosslinking Probabilities							
	0:0	1:11	1:6	2:7	4:9	6:11	2:3	1:1
		1	1	1	1..2	1..3	1..5	1
	1	2..5	2..3	2	3	4	6	
	2	6..9	4..5	3	4	5	7	
	3	10..11	6..7	4	5	6	8	
	4	14..17	8..9	5	6	7	9	
	5	18..21	10..11	6	7	8	10	
		22	12	7	8..9	9..10	11..15	2
Random number range	5	22	12	7	9	11	15	2

RESULTS

Representative consecutive structures, generated with a high and with a low probability of crosslinking and a time limitation of 80 megevents (million random movements) are shown in Fig. 2. Even though the sizes range from 60 to 227 monomer units, the lengths are fairly uniform. This is qualitative evidence that in a diffusion-limited process the active areas of growth are those points farthest from the center of gravity and that the rate of growth of the length of the structure is nearly constant. At low probability of crosslinking, occasional neighboring crosslinks were seen; at higher probability of crosslinking longer stretches of neighboring crosslinks occurred (see Fig. 2. for examples). The lengths of the two structures with crosslinking $p = 2:3$ (Fig. 2) are less than the lengths of the 5 structures with crosslinking $p = 1:11$. In Fig. 2 arrows point to two examples of chain termini that were programmed to be sterically excluded from end-to-end growth.

DISTRIBUTIONS. The scatter of size and length for 1200 simulations is shown in Fig. 3. The scatter exhibits no apparent repeating patterns, as might be expected from the random nature of Brownian motion. The scatter for length is much less than that for size and suggests that two different factors may be controlling the size and length of these structures. The distributions of size, length, width, and crosslinks for a large number of simulations at crosslinking $p = 1:11$ are presented in Fig. 4. Here the distribution of length is quantitatively seen to be much less than the distribution of size.

Distributions of properties of structures with crosslinking $p = 6:11$ as a function of time are characterized by polydispersity values in Table 2. The nearly equal polydispersities for radius of gyration and length are low and decrease sharply with increase in average size. In addition, they appear to converge as the average size of the

structures increases with time. The greatest polydispersity occurs with crosslinking, which property seems to control the polydispersity of width. The polydispersity of size falls between that for crosslinks and for length and decreases with time less sharply than that polydispersity for crosslinks.

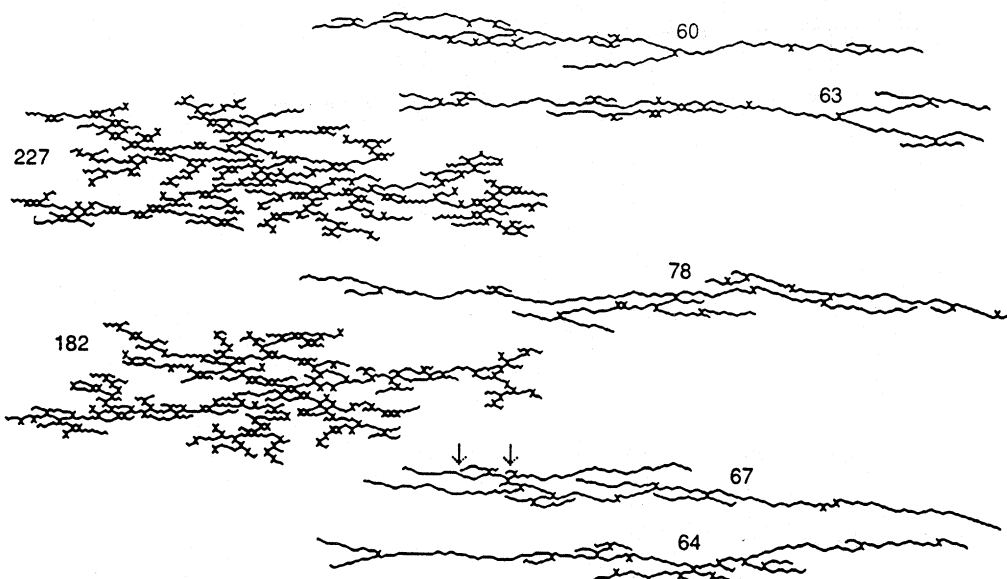


Fig. 2. Two 80 megevents simulations with crosslinking $p = 2:3$ (left) and five consecutive 80 megevents simulations with crosslinking $p = 1:11$, 68881 coprocessor.

Time. The logarithm of average value for size, length, width, radius of gyration, and crosslinks were best fitted by linear least squares to logarithm of time, measured in megevents. One typical set of results is shown in Fig. 5. The slopes and correlation coefficients are listed in Table 3. In general, the power law correlation coefficient was always greater than the coefficient obtained from simple linear regression. The slopes for average size and average number of crosslinks in Table 3 have nearly equal values. The slopes for length, width, and radius of gyration have values that are close to one another.

The growth of average properties with time at different crosslinking probabilities is shown in Fig. 6. The correlation coefficients in each instance were close to 1 and greater than correlation coefficients obtained from a linear least-squares fitting of average property to average time. These power law relationships result from the fractal properties of the structures. Because their properties fall into two groups of fractal dimensions (1.3 for size and crosslinks, and 0.7-0.8 for length, radius of gyration, and width, Table 3), the structures are multifractal. One significant consequence of this property is that, in macromolecular assemblies that are to any extent formed by a diffusion-limited process, the active sites for growth on the assembly are not uniformly distributed in solution, but rather have a fractal distribution.

Crosslinking. When no crosslinking is allowed, the growth of size and length is of course identical and follows a power law relationship with time (Fig. 6). In this special case the width is dependent only on the variation in orientation of the monomer attached end-to-end and can vary by no more than one unit per addition. When crosslinking is introduced, the growth of average size of the structures depends directly on the average number of crosslinks, as is shown in Fig. 7. However, the growth of the average width of the structures exhibits a power law dependency on the average number of crosslinks (Fig. 8); in addition, the slopes appear to be parallel. This suggests that a universal fractal dimension prevails for the growth of width and number of crosslinks. Not all crosslinks lead to an increase in width and this presumably accounts for the low value for the

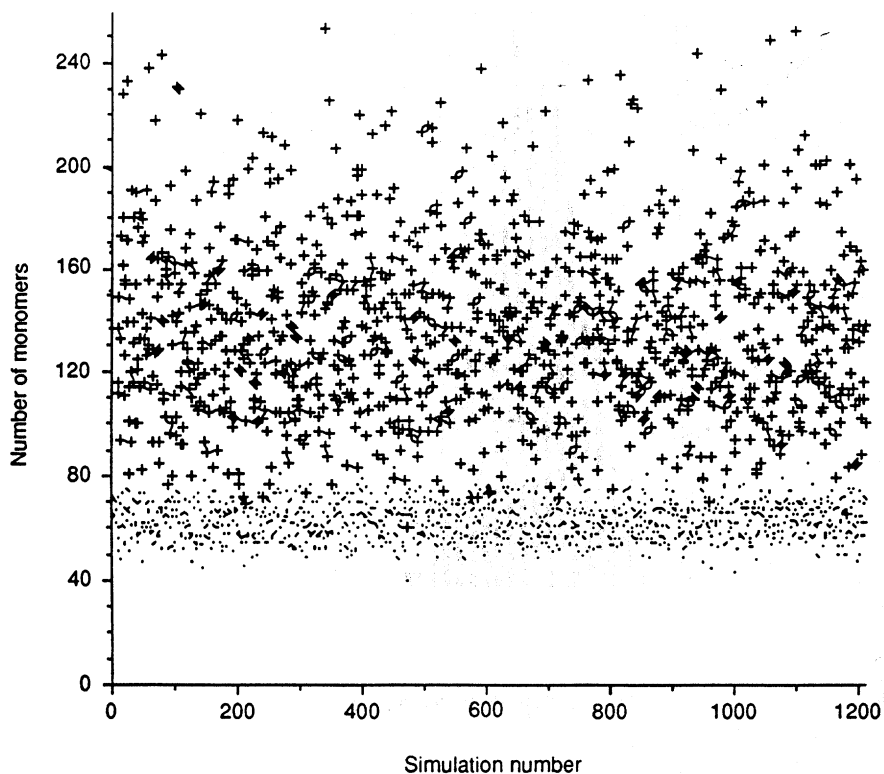


Fig. 3. Scatter of size (+) and length (·) of simulations, crosslinking $p = 1:6$, 50 megevents, 68881 coprocessor.

power law exponent. The dependency of width on crosslinking can explain the similar polydispersity values for width and for crosslinks in Table 2.

The dependency of growth of size on crosslinking is also depicted in Fig. 9 which relates power law exponents to probability of crosslinking. In the plots to the right can be seen the parallel increase in power law growth for both size and crosslinks. The exponents for radius of gyration and for length, in contrast, exhibit little variation with probability of crosslinking. The smaller exponents for growth of width increase with probability of crosslinking and point also to a relationship of growth of width to crosslinking. To the left in Fig. 9 are shown plots of power law exponents relating average radius of gyration, length, and width to average size. The exponents for both radius of gyration and length decrease at a decreasing rate with increasing probability of crosslinking and converge with the increasing exponents for width. At a crosslinking probability of 1, the power law relationship of radius of gyration, length, and width to size is similar (exponent = 0.55).

The power law exponents for growth of size rise with decreasing slope as the probability of crosslinking increases (Fig. 9). These exponents appear to converge with those for growth of average number of crosslinks at high probabilities of crosslinking (Fig. 9). At intermediate crosslinking probability there is some divergence between exponents for length and for radius of gyration. Also, at crosslinking $p > 0.5$ the power law exponent for growth of width with time seems to be constant.

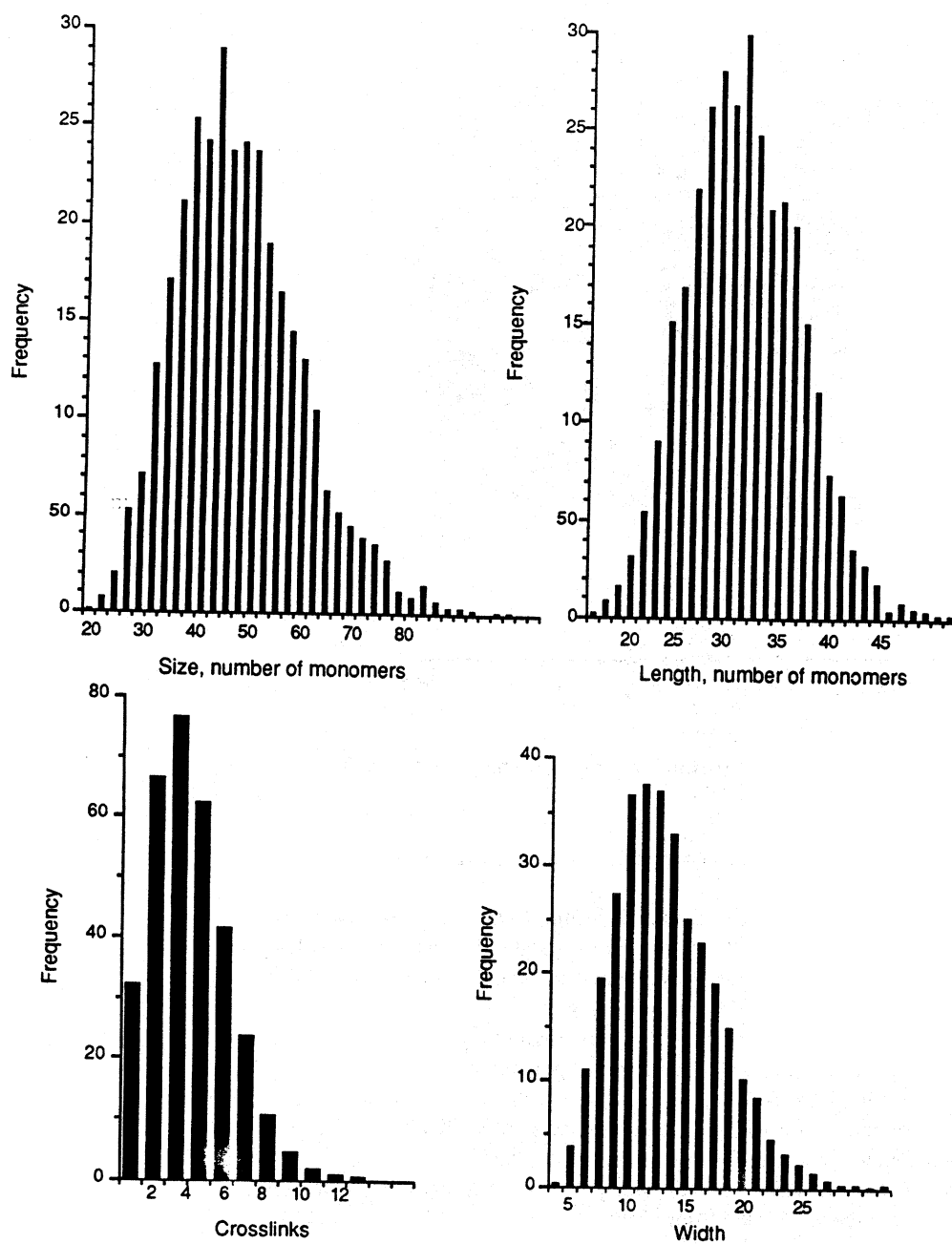


Fig. 4. Distributions of properties of 3203 simulations with crosslinking $p = 1:11$, 20 megevents, 8087 coprocessor.

Diffusion-limited aggregation of pectin

Table 2. Polydispersity^a of properties of 600 simulations with crosslinking p = 6:11, 68881 coprocessor.

megevents	R _g	size	length	width	crosslinks
10	1.02411	1.03731	1.02510	1.04044	1.05848
20	1.01404	1.02945	1.01299	1.03362	1.03829
30	1.00992	1.02419	1.00937	1.02793	1.03048
40	1.00753	1.02241	1.00677	1.02422	1.02628
50	1.00560	1.01821	1.00516	1.02113	1.02143
60	1.00528	1.01700	1.00480	1.01921	1.01915
80	1.00330	1.01658	1.00339	1.02048	1.01883

^aThe ratio of the root mean square average to the arithmetic average.

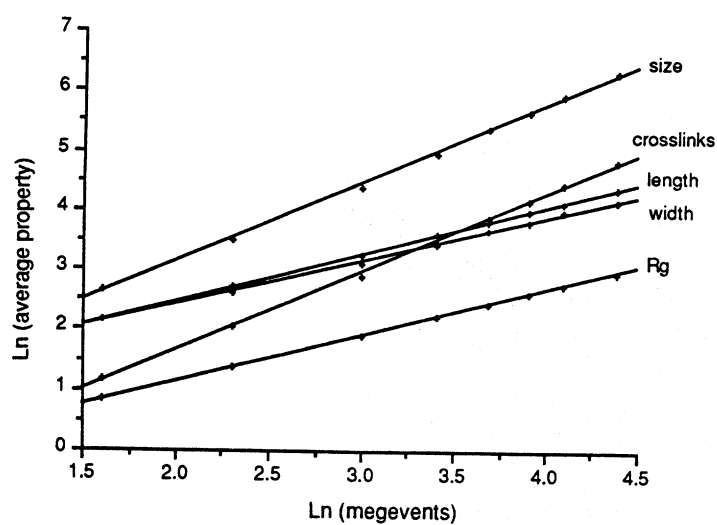


Fig. 5 Power law plots for average properties for 600 structures, crosslinking p = 1:6, 68881 coprocessor.

Table 3. Slopes and correlation coefficients (power law and linear) for simulations with crosslinking p = 6:11, 68881 coprocessor.

	size	crosslinks	length	width	R _g
Slopes, Fig. 5	1.3292	1.3223	0.8024	0.7360	0.7740
Correlation coefficient, Fig. 5	0.9993	0.9995	0.9999	0.9995	0.9999
Correlation coefficient simple linear regression	0.9917	0.9920	0.9972	0.9972	0.9963

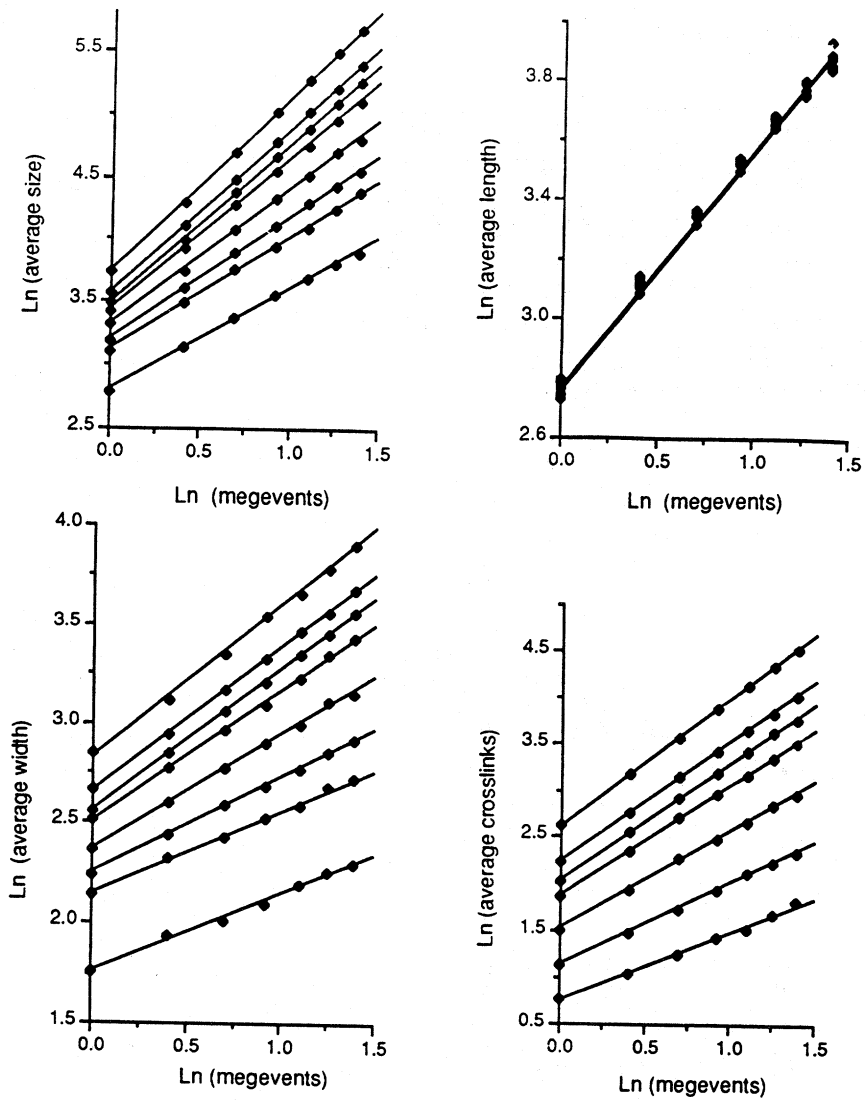


Fig. 6. Power relationship of growth of average size, length, crosslinks, and width of 600 structures (8087 coprocessor used for simulations). Crosslinking p , top to bottom: 1:1, 2:3, 6:11, 4:9, 2:7, 1:6, 1:11, 0:1 (not in crosslinks plot); slopes of the ln (average length) plots: 0:1, 0.803; 1:11, 0.808; 1:6, 0.772; 2:7, 0.773; 4:9, 0.780; 6:11, 0.781; 2:3, 0.792; 1:1, 0.801.

Diffusion-limited aggregation of pectin

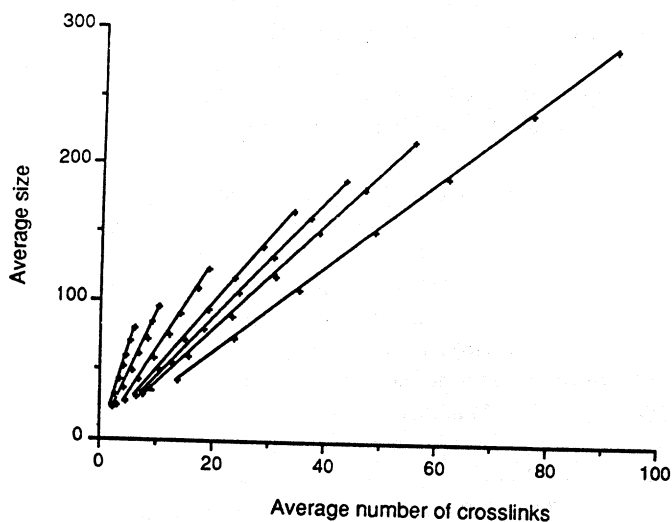


Fig. 7. Linear relationship between average number of crosslinks and average size at increasing megevents (8087 coprocessor). Crosslinking p from left to right: 1:11, 1:6, 2:7, 4:9, 6:11, 2:3, 1:1.

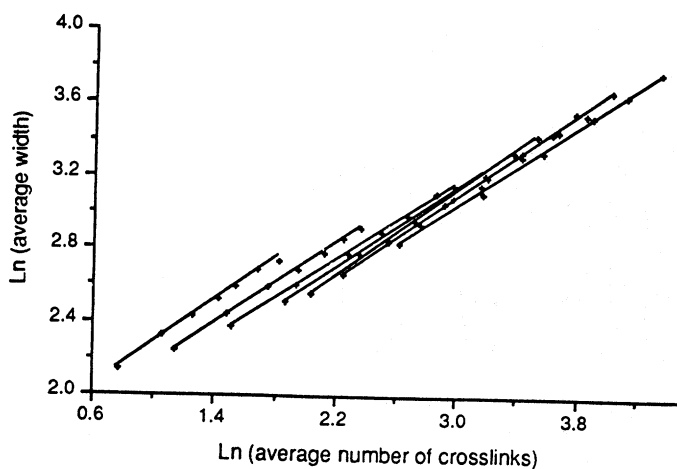


Fig. 8. Power law relationship between average number of crosslinks and average width, 600 structures, 8087 coprocessor, 15 to 40 megevents. Crosslinking p and (slope) from left to right: 1:11 (0.573); 1:6 (0.552); 2:7 (0.546); 4:9 (0.559); 6:11 (0.572); 2:3 (0.568); 1:1 (0.561).

Diffusion limitation. The power law plots of length versus time in Fig. 6 are remarkably parallel throughout the crosslinking probability range of 0.0 to 1.0. When the exponent, taken from the slopes of these plots, is plotted against crosslinking probability (Fig. 9), the points cluster around what might be a constant value (represented by the dashed line). The average length of these structures apparently is controlled by diffusion, or Brownian motion. As long as there is a steady supply of random walkers, the structures on the average will exhibit a uniform power law rate of growth under the full spread of probability of crosslinking. The consistent rate of growth of average length with time follows from the simulation condition that a random walker is always present within the bounding circle of the lattice. Thus, whenever a random walker attaches itself to a crosslinking site, a new random walker is introduced just within the bounding circle. Effectively, the random

walker bounces from a crosslinking site to a random position just within the bounding circle and thereby experiences just another random movement. The convergence of power law exponents relating average size to average radius of gyration, average length, and average width at a probability of crosslinking of 1 in Fig. 9 suggests that crosslinking has become at this point diffusion-limited. The new potential crosslinking sites are distributed away from the center of gravity in the same general area that contains ends of growing chains.

Shielding. The average properties of 600 structures after a set time interval are plotted against crosslinking in Fig. 10. The plots for average size and width are similar and curve downward at higher probability of crosslinking. In contrast, the average length decreases with increasing probability of crosslinking. With increasing probability of crosslinking the average number of crosslinks is nearly linear, but does exhibit slight upward curvature. These subtle effects may reflect shielding by these structures of free Brownian motion of the random walker. That is, on the average, a random walker that completes its path by attaching to a terminal zone would be impeded more by the larger structures that result from higher probability of crosslinking. This is one possible explanation for the decrease in average length in Fig. 10. At higher probability of crosslinking, a larger average number crosslinking sites would be formed at a greater distance from the center of gravity. This would account for the slight upward curvature of average crosslinks in Fig. 10. The falling off of increase in average size and width with increasing probability may also be ascribed to a general shielding effect of larger structures on the random walker. A future extension of the current simulation program would be to examine the effect of the lattice points made inaccessible to the random walker on the average properties of the structure.

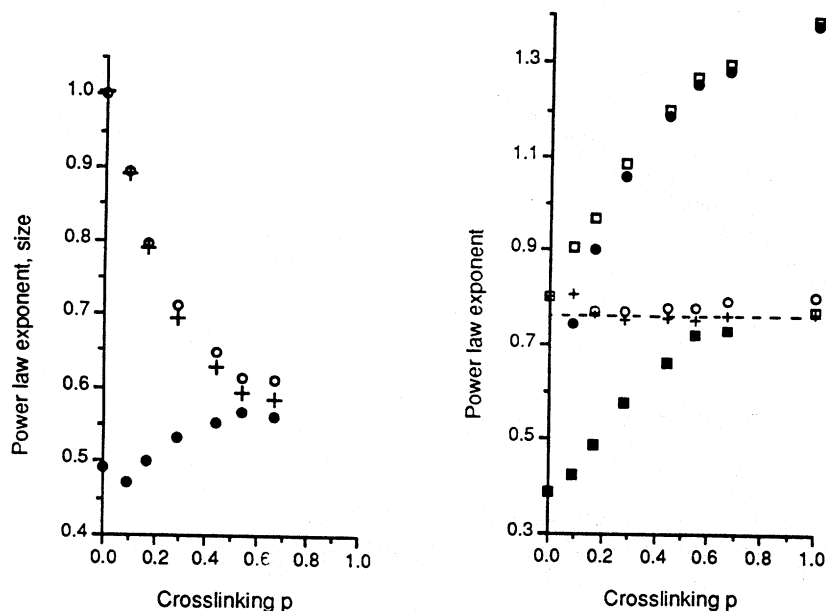


Fig. 9. Exponents from power laws that relate average properties of structures to growth of size (left: length, O; Rg, +; width, l) and to time in megevents (right: size, x; crosslinks, i; length, O; Rg, +; width, n), 8087 coprocessor.

Chain Distribution. The structures generated by the simulations can be viewed as assemblies of crosslinked chains (oligomers) of end-to-end joined monomers. The distribution of chain lengths in a given population of structures generated with a crosslinking probability of 1:1 is shown in Fig. 11. The distribution can be fitted by a power law. This is another fractal property of these structures.

At lower crosslinking probabilities a corresponding power law was not found. The shorter chains exhibited a higher frequency that reflects shielding. That is, short chains near the center of gravity are effectively shielded from monomers by more active sites near the ends of the structures. In the case of high crosslinking-probability-structures, most of the shorter chains are located away from the center of gravity and are maintained in a more active environment inasmuch as they have a higher probability of encountering a random walker. As the structure grows, the sites for possible attachment of monomer change their reactivity. Reactivity of these sites is keyed to physical factors such a distance from the center of gravity and relative position within the structure.

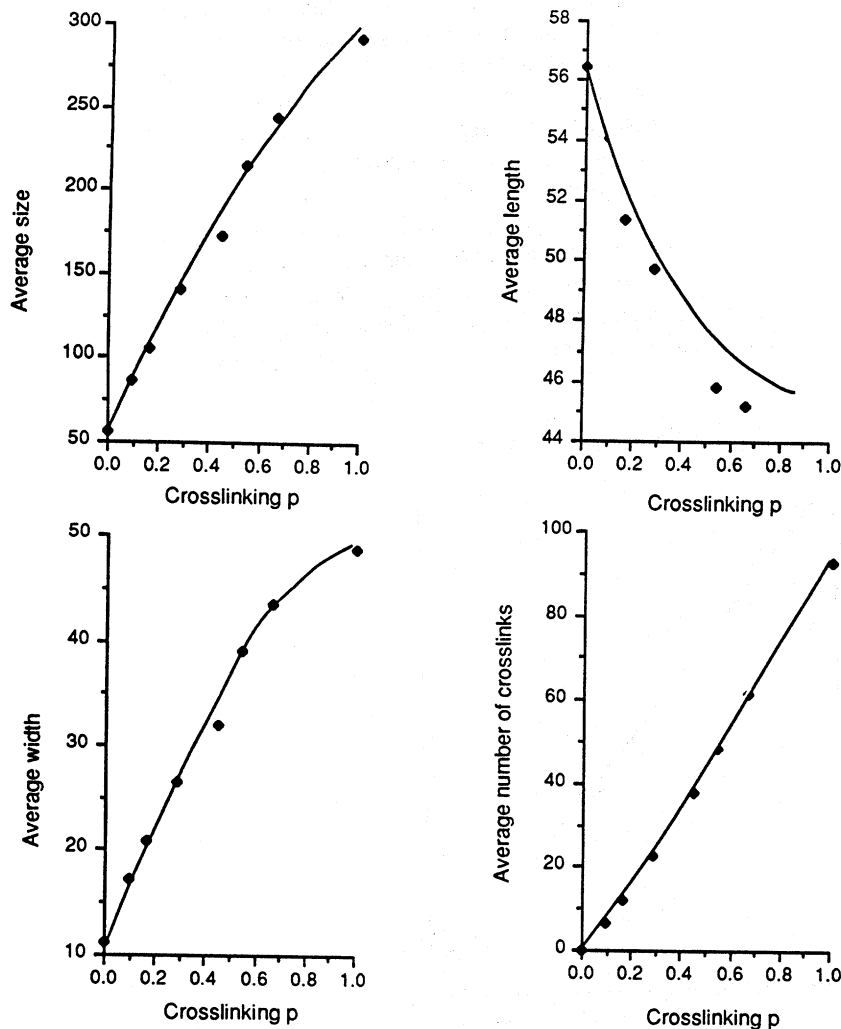


Fig. 10. Average properties of 600 structures after 40 megevents plotted against crosslinking p, 60881 coprocessor.

Real Simulation Times. The real time that a random walker resided within a given bounding circle was averaged over the number of simulations performed under a given set of conditions. This time was measured by the number of tics (1/60th of a second, 68881 coprocessor) between the initiation of a random walk and the completion of the walk on arrival at a permanent site on the lattice. The average time that a structure spends in a given bounding circle is directly related to the number of lattice points encompassed by the circle as

shown in Fig. 12. This relationship follows from the fractal dimension of 2 for Brownian motion on a square lattice. This plot also makes possible the estimation of time required to produce average structures of given length and given megevents. This information is useful for establishing practical upper limits for simulation sizes. In the present study, 600 simulations within a range of from 5 to 80 megevents with a 720 x 720 square lattice could be carried out with a 68881 coprocessor at 16 MHz within two weeks.

Pectin Aggregation. The simulations reported herein produce classes of fractal shapes. The factors of diffusion and crosslinking which govern the properties of these classes of shapes can be applied in three dimensions to aggregates of pectin. For example, segmented rod pectin monomers could form large aggregates through end-to-end interactions at terminal junction zones. Limited crosslinking would favor extension into three dimensions without the formation of precipitates. The process of cluster aggregation, not covered by these simulations, could then lead to gel formation whenever the aggregate size and number pass a critical point.²⁵⁻²⁶ A junction zone of pectin is considered to be a block of polygalacturonate, some 20-30 units long (9 - 12 nm). Under some conditions these blocks assume a three unit per turn helical conformation in which every third carboxyl group projects out from and coplanar with the axis²⁷. Such a set of carboxyl groups is thought to interact co-operatively with a similar set of carboxyl groups in a junction zone of another pectin monomer to give aggregation or gelation.¹⁸ The simulation model used for this first study assumes a minimal pectin monomer with only three junction zones (MW ca. 15,000).²⁸ Simulation structures of size 100 would give pectin aggregate sizes of 1.5 million, which is well within some of the upper limits of molecular weights reported in the

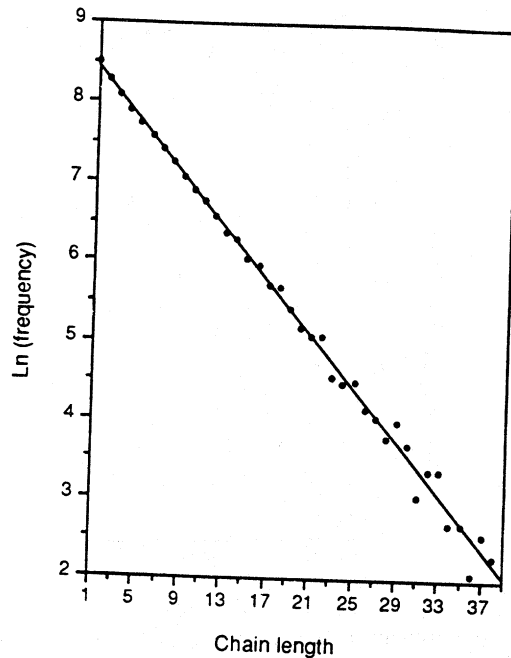


Fig. 11. Power law relationship of frequency of chains to chain length, crosslinking $p = 1:1$.

Diffusion-limited aggregation of pectin

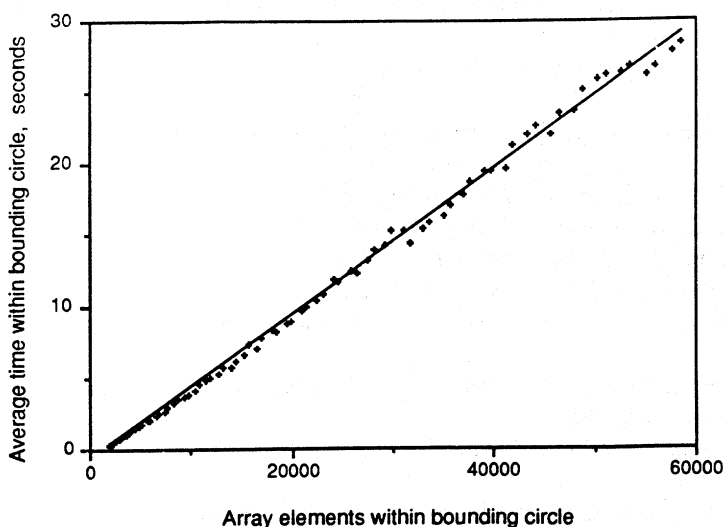


Fig. 12. Average real time that random walker moved among lattice points within bounding circle; 80 megevents, crosslinking $p = 6:11$, 68881 coprocessor.

literature.²⁹ Large pectin macro-assemblies, that have been assigned shapes such as a sphere, rod, random coil, or segmented rod, have been employed with limited success to determine size and molecular weight from the diffusion coefficient, determined by dynamic light scattering.²⁹ The fractal shapes provided by simulation of diffusion-limited aggregation offer what might now be regarded as more realistic shapes for relating diffusion coefficients to other solution properties of pectin. Under experimental conditions that allow measurement of molecular weight, or size and radius of gyration of fractal aggregates, a power law relationship between MW and R_g can be anticipated.

Our current understanding of the special reactivity of chain ends in diffusion-limited aggregation, suggests that a further refinement of the present simulation model would be to allow crosslinking by end-to-internal zone interactions, so that chains would be linked to each other at branch points. This follows from the consideration that internal zone-internal zone contact is expected to be less favored by diffusion than end-to-internal zone approaches. This could very likely be demonstrated by actual simulations that incorporate these possibilities.

One significant contribution these simulations make to our understanding of pectin aggregation is that the new fractal geometric shapes generated can influence in a concrete way our concepts of how such aggregates might appear. Moreover, the distributions of the average properties of these shapes are similar to the respective distributions of properties of polymers in general. The simulation model can be modified readily according to the rules that polymer chemists have found for the association of monomers.

REFERENCES

1. Mandelbrot, B. B. *The Fractal Geometry of Nature* Freeman: San Francisco, 1982.
2. Halsey, T. C.; Meakin, P. "Axial Inhomogeneity in Diffusion-Limited Aggregation". *Phys. Rev. A: Rap. Comm.* **1985**, *32*, 2546-2548.
3. Jullien, R.; Botet, R. *Aggregation and Fractal Aggregates*, World Scientific: Singapore, 1987.
4. Kolb, M.; Botet, R.; Jullien, R. "Scaling of Kinetically Growing Clusters". *Phys. Rev. Lett.* **1983**, *51*, 1123-1126.
5. Kolb, M.; Jullien, R. "Chemically Limited Versus Diffusion-Limited Aggregation". *J. Physique Lett.* **1984**, *45*, L-977-L-981.

6. Meakin, P. "Formation of Fractal Clusters and Networks by Irreversible Diffusion-Limited Aggregation". *Phys. Rev. Lett.* **1983**, *51*, 1119-1122.
7. Witten, T. A., Jr.; Sander, L.M. "Diffusion-Limited Aggregation, a Kinetic Critical Phenomenon". *Phys. Rev. Lett.* **1981**, *47*, 1400-1403.
8. Weitz, D. A.; Huang, J. S.; Lin, M. Y.; Sung, J. "Limits of the Fractal Dimension for Irreversible Kinetic Aggregation of Gold Colloids". *J. Phys. Rev. Lett.* **1985**, *54*, 1416-1419.
9. Weitz, D. A.; Lin, M. Y.; Sandroff, C. J. "Colloidal Aggregation Revisited: New Insights Based on Fractal Structure and Surface-Enhanced Raman Scattering". *Surf. Sci.*, **1985**, *158*, 147-164.
10. Matsushita, M.; Sano, M.; Hayakawa, Y.; Honjo, H.; Sawada, Y.; "Fractal Structures of Zinc Metal Leaves Grown by Electrodeposition". *Phys. Rev. Letters*, **1984**, *53*, 286-289.
11. Rees, D. A. "Polysaccharide Conformation in Solutions and Gels - Recent Results on Pectins". *Carb. Polym.* **1982**, *2*, 254-263.
12. de Vries, J. A.; Hansen, M.; Söderber, J., Glahn, P. E.; Pedersen, J. K. "Distribution of Methoxyl Groups in Pectins". *Carb. Polym.*, **1986**, *6*, 165-176.
13. Oakenfull, D.; Scott, A. "Hydrophobic Interaction in the Gelation of High Methoxyl Pectins". *J. Food Sci.*, **1984**, *49*, 1093-1098.
14. Smidrød, O.; Haug, A. "Properties of Poly(1,4-Hexuronates) in the Gel State. II. Comparison of Gels of Different Chemical Composition". *Acta Chemica Scand.*, **1972**, *26*, 79-88.
15. Thibault, J. F.; Rinaudo, M. "Gelation of Pectinic Acids in the Presence of Calcium Counterions". *Brit. Polm. J.*, **1985**, *17*, 181-184.
16. Northcote, D. H. "Chemistry of the Plant Cell Wall". *Ann. Rev. Plant Physiol.*, **1972**, *23*, 113-132.
17. Kohn, R. "Ion Binding of Polyuronates - Alginate and Pectin". *Pure Appl. Chem.* **1975**, *42*, 371-397.
18. Rees, D. A.; Wight, A. W. "Polysaccharide Conformation. Part VII. Model Building Computations for α -1,4 Galacturonan and the Kinking Function of L-Rhamnose Residues in Pectic Substances". *J. Chem. Soc.* **1971**, 1366-72.
19. Plaschina, I. G.; Semenova, M. G.; Braudo, E. E.; Tolstoguzov, V. B. "Structural Studies of the Solutions of Anionic Polysaccharides. IV. Study of Pectin Solutions by Light-Scattering". *Carb. Polm.* **1985**, *5*, 159-179.
20. Fishman, M. L.; Gross, K. C.; Gillespie, D. T.; Sondey, S. M. "Macromolecular Components of Tomato Fruit Pectin" *Arch. Biochem. Biophys.* **1989**, *274*, 179-191.
21. Fishman, M. L.; El-Atawy, Y. S.; Sondey, S. M.; Gillespie, D. T.; Hicks, K. B. "Component and Global Average Raddii of Gyration of Pectins from Various Sources" *Carb. Polymers*, **1990**, in press.
22. Meakin, P. "Simulations of Aggregation Processes". in Avnir, D.; ed, *The Fractal Approach to Heterogeneous Chemistry: Surfaces, Colloids, Polymers*, John Wiley: New York, 1989.
23. Porter, K. "Handling Huge Arrays". *Dr. Dobb's J. Software Tools*, **1988**, *13*, 108-115.
24. Flory, P. J. *Statistical Mechanics of Chain Molecules*, Interscience: New York, 1969.
25. Kolb, M. "Reversible Diffusion-Limited Cluster Aggregation". *J. Phys. A: Math. Gen.* **1986**, *19*, L263-L268.
26. Kolb, M.; Herrmann, H. J. "The Sol-Gel Transition Modelled by Irreversible Aggregation of Clusters". *J. Phys. A: Math. Gen.* **1985**, *18*, L435-L441.
27. Walkinshaw, M. D.; Arnott, S. "Conformations and Interactions of Pectins. I. X-ray Diffraction Analyses of Sodium Pectate and Neutral and Acidified Forms". *J. Mol. Biol.* **1981**, *153*, 1055-1073.
28. Fishman, M. L.; Pepper, L.; Damert, W. C.; Phillips, J. G.; Barford, R. A. "A Critical Reexamination of Molecular Weight and Dimensions for Citrus Pectins" in Fishman, M.L.; Jen, J.; ed. *Chemistry and Function of Pectin*, ACS Symposium Series 310, Washington, DC, 1986.
29. Chapman, H. D.; Morris, V. J.; Selvendran, R. R.; O'Neill, M. A. "Static and Dynamic Light-Scattering Studies of Pectic Polysaccharides from the Middle Lamellae and Primary Cell Walls of Cider Apples" *Carb. Res.* **1987**, *165*, 53-68.